

Review of tomographic methods

Bernard Law and Daniel Trad

ABSTRACT

Classical reflection travel-time tomography can accurately estimate the subsurface velocity; however, the difficulties in picking reflection arrival times on continuous events on CDP stacks and unmigrated gathers make this an undesirable approach. Over the past 30 years, reflection tomography has been extended to estimate other attributes, such as anisotropic parameters and attenuation. Automatic picking of residual moveouts on common image gather in prestack depth migrated domain also improves the picking efficiency. Stereotomography characterizes any reflection event by its two-way travel-time and the apparent slopes or ray parameters in shot and received gathers; hence, does not require picking along continuous reflector. Besides improving the picking efficiency, stereotomography also uses the apparent slopes of coherent reflection events, in addition to the travel-times, in the inversion process. In this study, we review the classical reflection tomography, prestack depth migration tomography, and stereotomography, and to compare the advantages and disadvantages of each method.

INTRODUCTION

Tomography is from the Greek word “*tomos*” meaning “section” or “slice” (Bording et al., 1987; Lines and Newrick 2004) and “*graphia*” meaning “describing”. Thus, tomography is a process that describes the material properties within the body of investigation. Seismic tomography methods share some similar physical and mathematical principles with medical tomography. Both methods seek to determine the interior distribution of values of physical properties (the integrant) from the projections (the integral or the sums of some interior value) measured outside of an object (Steward 1991). In seismic travel-time tomography seismic energy propagated through the medium and are received at the receivers on the surface or in the borehole:

$$t_{raypath} = \int_{raypath} s(x, z) dl, \quad (1)$$

where the measured travel-time t is the integration of $s(x, z)dl$, along the ray path. The objective of travel-time tomography is to determine the integrant $s(x, z)$, the slowness of the medium. Therefore equation 1 represents the forward modeling of the travel-times, and the solution of $s(x, z)$ represents the solution of the inversion problem.

In classical reflection travel-time tomography (Bishop et al., 1985, Chiu and Steward, 1987) the data space of the inversion problem is represented by the difference between the picked and modelled reflection travel-time of the primary reflection events on the CDP stacks and CDP gather. The model space includes the slowness model and reflection boundaries, and the effects of the two can be too hard to separate (Stork and Clayton, 1985, 1991; Gray et al., 2000). Iterative migration and reflection tomography method (Bording et al., 1987) used travel-time tomography to update the velocity model only. Reflection boundaries were updated using post-stack depth migration. The migrated image was tied

with available well logs, until well ties were satisfactory. Stork and Clayton (1991) included the reflection position in the reflection tomography step and followed the reflection tomography step with post-stack migration. The iteration would stop when there was no change in the velocity model. Although travel-time tomography can produce theoretically accurate results; the picking of unmigrated travel-time along coherent reflectors can be tedious. This becomes more difficult in areas of structural complexity.

The 1990s have seen many developments in prestack depth migrated (PSDM) tomography (Woodward et al., 2008). PSDM tomography (Stork, 1992; Wang, 1995; Etgen, 2002) used the residual moveout within migrated common image gather (CIG) to update the velocity. CIG is often also referred to as common reflection gather (CRG). Since reflection energy is more coherent in the CIG than unmigrated gathers, automatic picking of residual moveout and dip is possible using windowed semblance (Etgen, 2002). Most PSDM tomography required linear velocity inversion (Adler 2008), because the reconstructed travel-time is not invariant and would require a prestack migration cycle for each velocity model update (Figure 1a). Adler (2008) introduced non-linear PSDM tomography where the migration velocity model is decoupled from the tomographic inversion velocity model and the invariant is the depth of the reflection event in a CIG. This allowed the velocity model to be updated and residual recomputed iteratively. This eliminated the requirement of PSDM cycle between iterations (Figure 6b).

Stereotomography methods include CDR tomography (Sword 1987), stereotomography (Billette et al. 1998, 2003), and adjoint stereotomography (Tavakoli 2017). These methods used two-way travel-times and apparent velocity (ray parameter) in the shot and receiver domains to fully characterize a locally coherent reflection or diffraction segment and tie it to a pair of rays and a scatter in depth. This approach eliminated the requirement of picking along continuous events; hence, making automated picking easier than the classical reflection tomography (Billette, 2003). Furthermore, travel-times and slopes of these locally coherent events are used in stereotomography methods. However, for noisy data and in areas of complex structure, picking can still be a challenge. Chauris et al. (2002) proposed a method to characterize a locally coherent event in depth migrated domain by its position in depth (x,z), half offset (h), dip (ξ) in migrated common offset gather and residual moveout (ϕ) in the CIG at (x,z,h). This is equivalent to stereotomography in depth, because data space parameters are measured in depth and can be more effectively in noise area.

Guillaume (2008) proposed a method to de-migrate a residual moveout pick on CIG to pre-migration invariant data: a source position, a receiver position, the travel-time and travel-time gradient. These invariant data are independent of migration velocity model. The collection of these invariant data was used to predict new residual moveout by kinematic re-migration. The new residual moveouts were used to invert for new velocity. This is iterated until the residual moveout is minimized. This approach does not require PSDM between each velocity model update.

We will review the classical stereotomography, PSDM tomography and stereotomography, and compare their advantages and disadvantages.

THEORY

Linear inversion

The line integral equation (1) can be represented in matrix form as:

$$\mathbf{t} = \mathbf{L} \mathbf{m} . \quad (2)$$

where \mathbf{L} is a matrix where a row contains the ray path segment length for each cell for a ray path. The cost function for equation 2 is:

$$J(s) = \| \mathbf{t}^{obs} - \mathbf{L} \mathbf{s} \|^2 \quad (3)$$

Non-linear inversion

For non-linear problem, ray path is a function of the slowness and equation (2) becomes:

$$\mathbf{t} = \mathbf{L}(\mathbf{s}), \quad (4)$$

and the cost function for equation 4 is:

$$J(s) = \| \mathbf{t}^{obs} - \mathbf{L}(\mathbf{s}) \|^2 \quad (5)$$

Since t^{obs} is picked from the data; it is invariant or model independent. We can exactly calculate the cost function in equation (5). Therefore, the non-linear problem of classical reflection tomography can be linearized by iteratively solving:

$$\Delta \mathbf{t} = \mathbf{L} \Delta \mathbf{s}, \quad (6)$$

where $\Delta \mathbf{s}$ is the model update vector between iterations, \mathbf{L} is the Frechét derivative matrix $\partial L(s)/\partial s$, the partial derivatives of the modelled response with respect to the model parameters and $\Delta \mathbf{t}$ is the differences between the modelled response and the observed data. Equation (5) can be written for a non-linear system as:

$$\Delta \mathbf{s} = (\mathbf{L}^T \mathbf{L})^{-1} \mathbf{L}^T \Delta \mathbf{t} \quad (7)$$

Classical reflection tomography

The classical reflection tomography method (Bishop,1985) involves picking reflection travel-times of a coherent continuous event on CDP stack and CDP gathers. The predicted travel-times can be computed by shooting rays from the picked and updated reflection boundaries to the surface (Figure 1a). The objective of this method is to estimate the model parameters by minimizing the difference between observed and predicted pick travel-times using equation (6) or (7) (Figure 1b-1c).

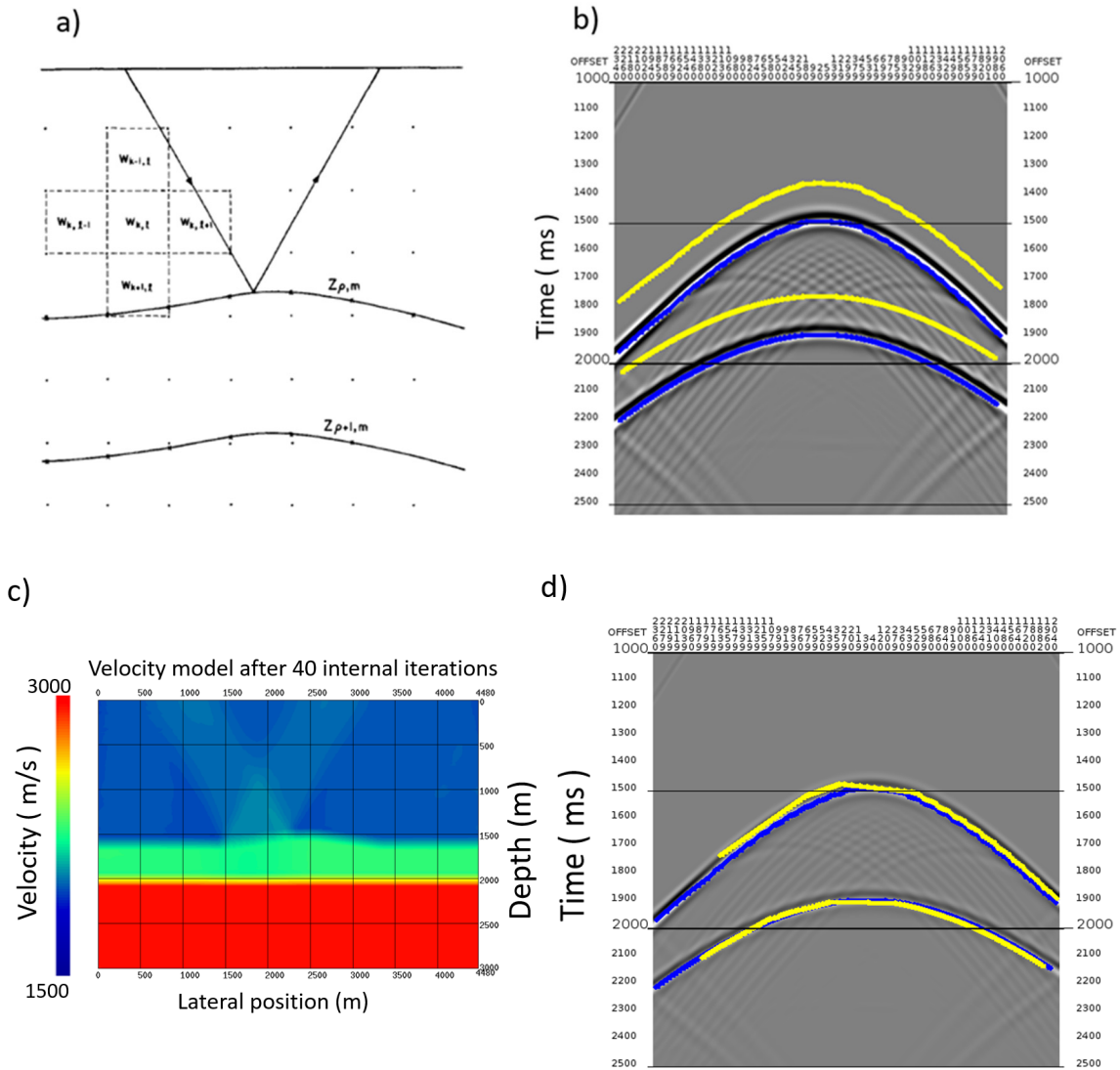


Figure 1. a) Velocity grid and reflection boundaries. (From Bishop 1985). b) Synthetic shot gather with predicted travel-time picks with the wrong velocity model (yellow) and with the correct velocity model (blue). c) Final velocity model after 40 iterations. d) predicted travel-time picks (yellow) using the updated velocity model (c).

The model space of this method includes the slowness model and reflection boundaries, and the effect of the two can be too hard to separate. To address the difficulties in separating velocity and reflection boundary updates, Bording et al. (1987) separated the reflection boundary from velocity inversion and followed the velocity update with post-stack migration to update reflection boundaries (Figure 2). Stork and Clayton (1991) proposed to invert for velocity and depth simultaneously and to pick the new reflection boundaries after re-migration with the new velocity model.

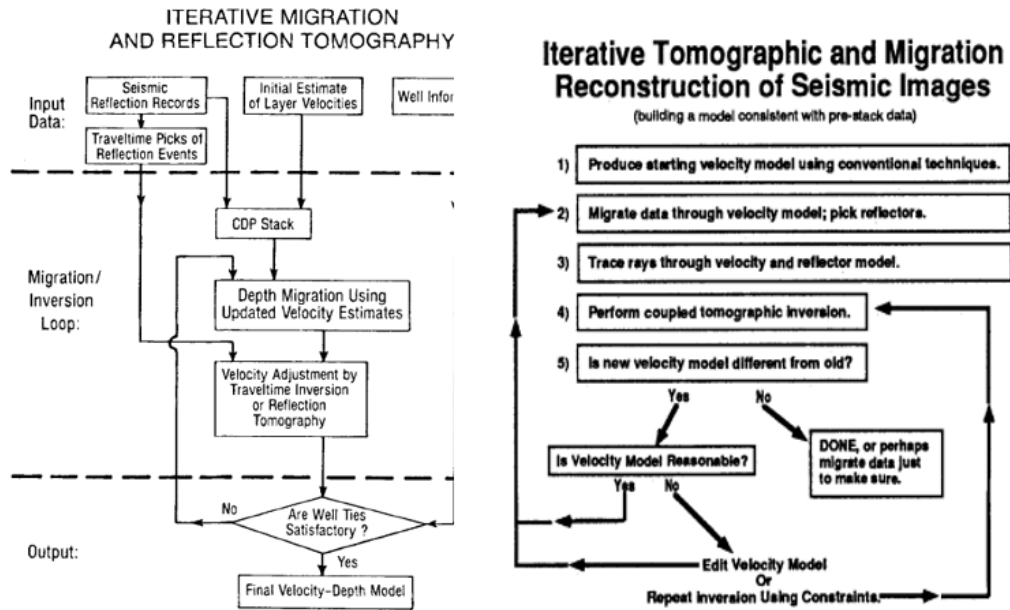


Figure 2. Iterative migration and reflection tomography flow charts from Bording et al. (1987) and Stork and Clayton (1991)

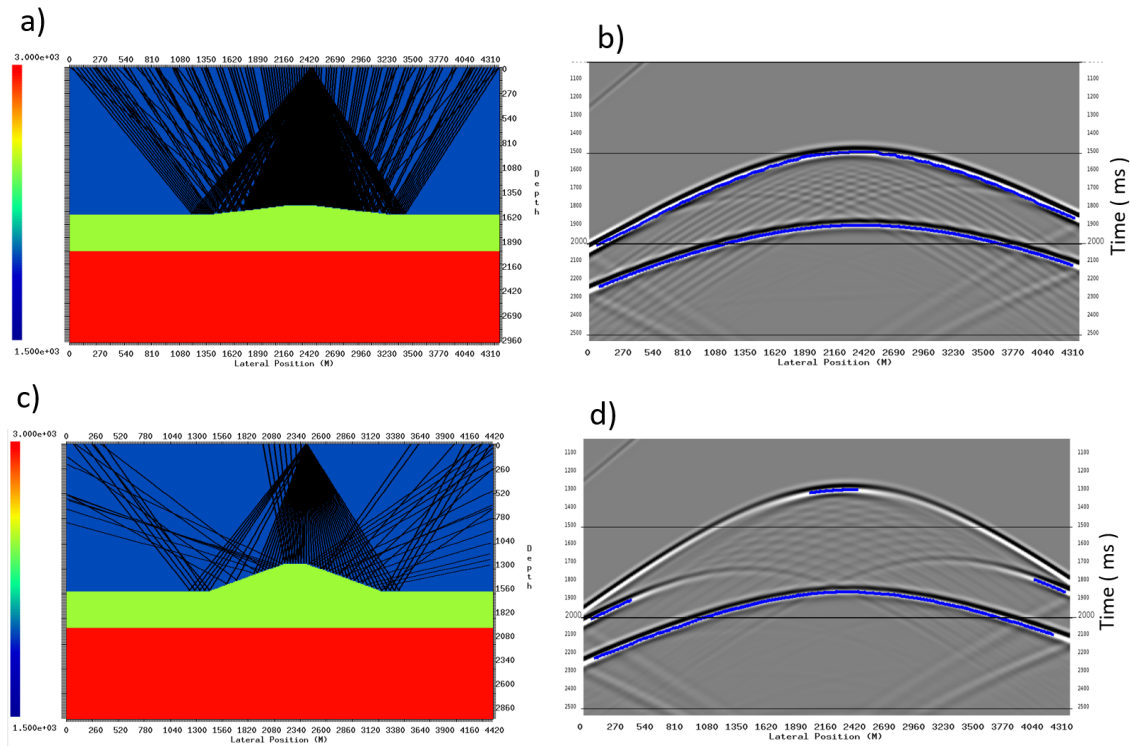


Figure 3. a) Ray paths from a velocity model with a small structural anomaly. b) predicted reflection travel-times (in blue) from the two reflection interfaces. c) ray paths after the dip of the structural anomaly is increased. d) predicted reflection travel-times (in blue) from the two reflection interfaces.

Another problem faced by the classical reflection tomography is that both the picking and ray tracing becomes difficult in more structurally complex area. Figure 3a shows the ray paths of a velocity model with a simple structure anomaly. There are some overlapping ray paths between reflection from the flat reflection boundary and the ray paths from the dipping reflection boundary. Figure 3b shows that the predicted reflection travel-times (in blue) agree with the finite difference modelled data. However, when the dip of the structural anomaly increases, more reflected ray paths from the dipping reflection boundary overlap with the ray paths from the flat reflection boundary. For this reason and because of the possibilities that computing power brings, other methods such as PSDM tomography and stereotomography have been developed and used to alleviate the limitation of picking of prestack data and ray tracing.

PSDM tomography

Al-Yahya (1989) showed that the post-migration depth z_m is related to the true depth z by:

$$z_m = \sqrt{\gamma^2 z^2 + (\gamma^2 - 1)x^2} \quad (8)$$

where $\gamma = \frac{w}{w_m}$, with w being the true average slowness and w_m being the average slowness used in the migration. This allows residual depth errors to be determined by semblance scanning using equation 8. Figure 4a shows CRG gathers with true velocity, slow velocity, and fast velocity. Figure 4b shows the γ scan of the

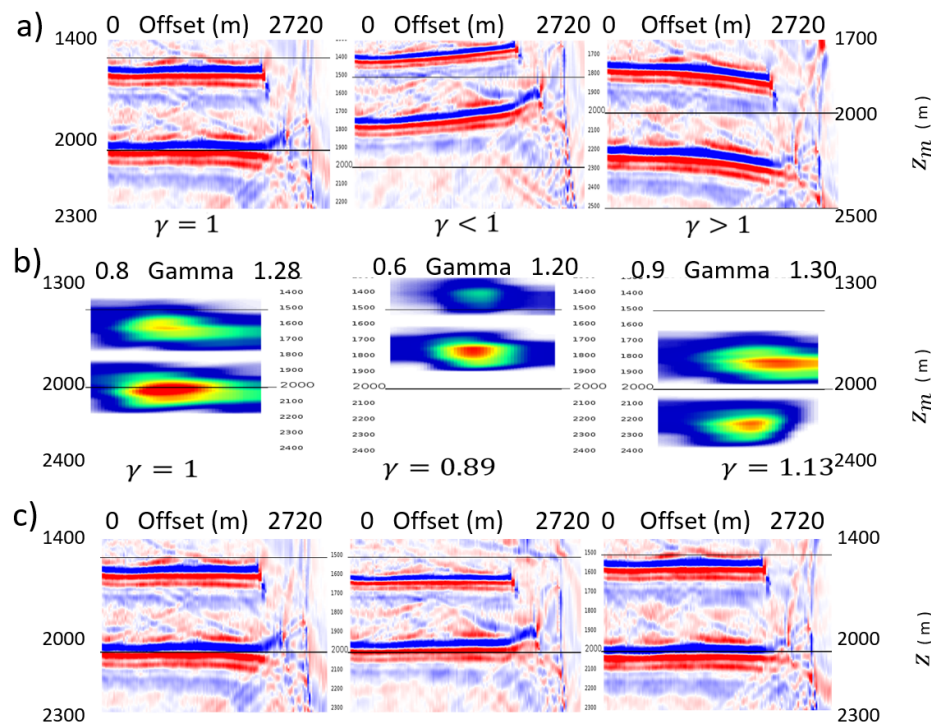


Figure 4. a) CRG gathers with true velocity, slow velocity, and fast velocity. b) Gamma scan of (a). c) application of gamma picks to (a).

corresponding CRG. Figure 4c shows the CRG after correction using the γ values and equation.

Slowness model and reflector interface update is possible using γ . Gray (2000) back-projects the velocity correction along the ray paths to update the velocity model (figure 5a). Stork (1990,1991) uses ray path geometry (figure 5b) to show that:

$$\Delta t = (a + b) \cdot s, \quad (9)$$

$$\Delta t = 2 \cdot s \cdot dh \cdot \cos(\theta), \quad (10)$$

$$\Delta t = 2 \cdot s \cdot \Delta z \cdot \cos(\phi) \cdot \cos(\theta), \quad (11)$$

where a and b are the extra distances travelled due to depth deviation caused by the changes in slowness, dh is the perpendicular distance between the old and new refractor position, ϕ is the dip angle of the refractor and θ is the incident angle of the reflection ray path. Hence equation (6) can be express as:

$$L \Delta s = 2 \cdot s \cdot \Delta z \cdot \cos(\phi) \cdot \cos(\theta), \quad (12)$$

and Δs can be solved iteratively using Δz computed from the gamma scan, incident angle computed from previous ray tracing steps and dip angles computed from reflection boundary picked from the migration step from the previous iteration.

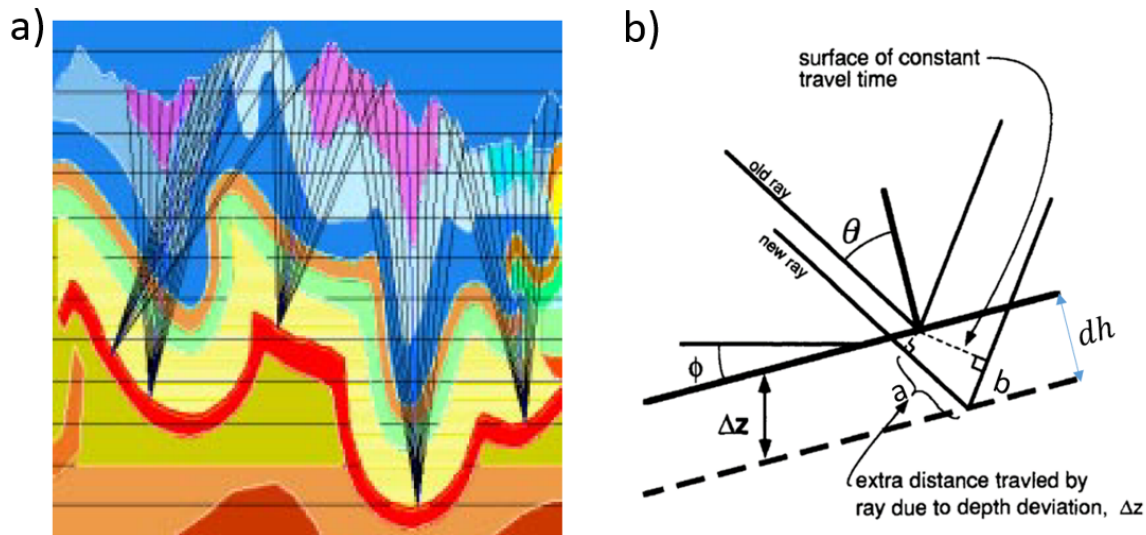


Figure 5. a) Back project velocity correction along ray paths (Gray 2000) b) Ray path geometry showing how Δz is converted to Δt (Stork 1991,1992)

Linear PSDM tomography

PSDM tomography uses the residual moveout within migrated CRG to update the velocity by minimizing the residual depth errors in the CRG gathers. Since reflection energy is more coherent in the CRG than unmigrated gathers, automatic picking of residual moveout and dip is possible using windowed semblance. The objective of PSDM is to estimate the velocity update by minimizing the objective function:

$$J(s) = \| \mathbf{t}^{obs} - \mathbf{t}(m) \|^2 \quad (13)$$

t^{obs} is approximated by using new estimated imaged depth $z(h, m) = z(h_0, m) + \Delta z(h, m)$; therefore, it is not an invariant. Since this is only an approximation; the cost function cannot be computed exactly, and the inversion cannot be linearized iteratively. The model update computed by this approach must be applied linearly and a PSDM cycle is required for each model update.

Non-linear PSDM tomography

Adler (2008) introduced a non-linear PSDM tomography where migration velocity model, m_G and tomography velocity model, m , are decoupled. The cost function for the inversion is:

$$J(m) = \| Z_G^{obs}(h, m_G) - Z_G(h, m) \|^2, \quad (14)$$

$Z_G^{obs}(h, m_G)$ is the depth of reflection event at half offset, h , in a CRG. It is invariant or independent of tomography model m . $Z_G(h, m)$ is modelled depth using tomography model m . This allows tomography model m to be updated and residual recomputed iteratively. This eliminates the requirement of PSDM cycle between iteration (Figure 1b).

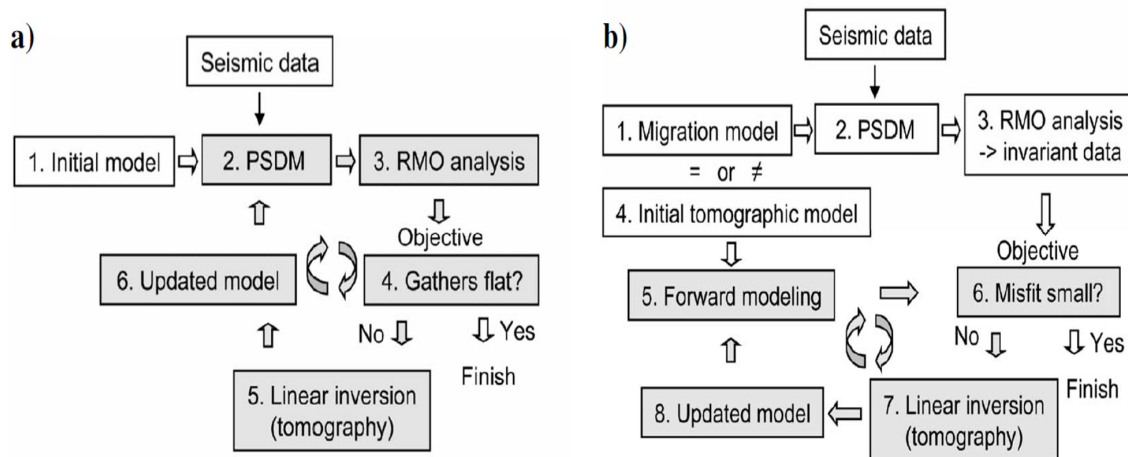


Figure 6 (a) Linear PSDM tomography. (b) Nonlinear PSDM tomography (From Adler 2008)

Stereotomography

Stereotomography methods (Figure 7) include CDR tomography (Sword 1987), classical stereotomography (Billette 1998,2003) and adjoint stereotomography (Tavakoli 2017), use two-way travel-times and apparent velocity (ray parameter) in the shot and receiver domains to fully characterize a locally coherent reflection or diffraction event (Figure. 8). Two-way travel-times and apparent velocities can be picked on the semblance of the localized shot and receiver slant stacks (Figure 9). This approach eliminates the requirement of picking along continuous events; hence, making automated picking easier than the classical reflection tomography. However, for noisy data and in areas of complex structure, picking can still be a challenge.

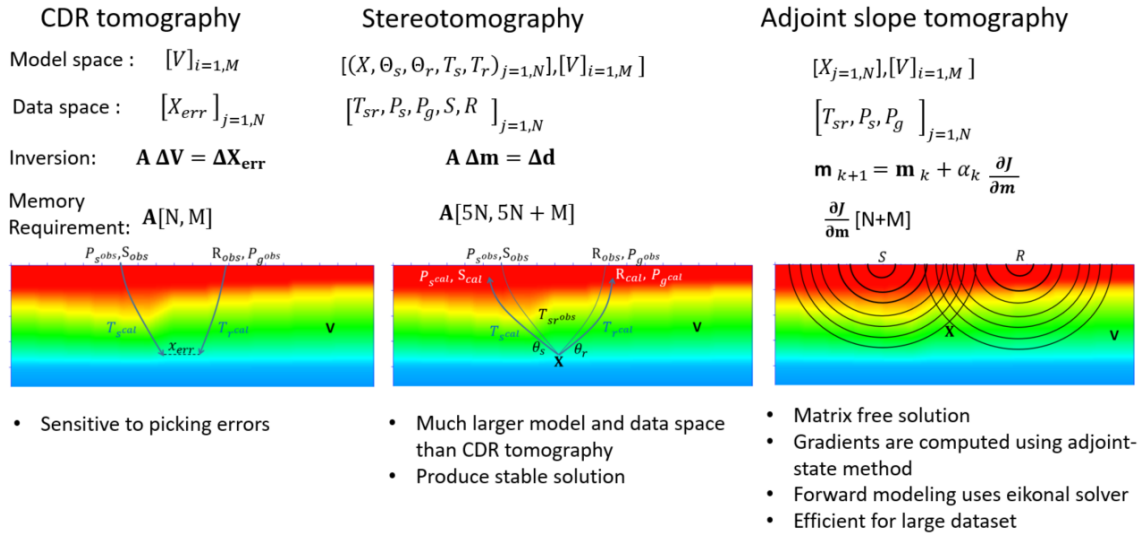


Figure 7: Stereotomography methods

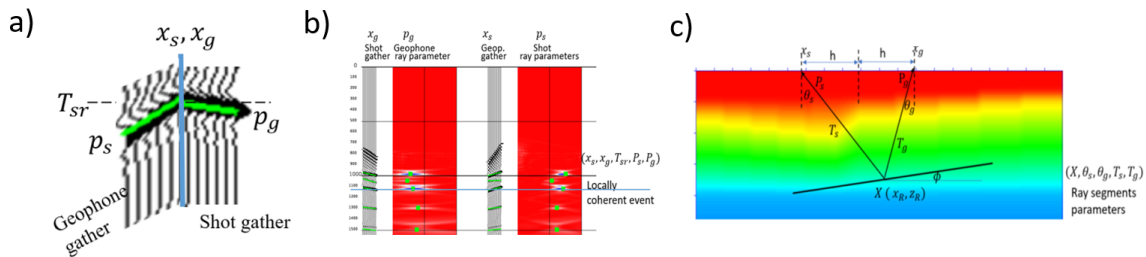


Figure 8 (a) Relationship between T_{sr}, P_s, P_g . (b) A locally coherent event can be picked on the localized shot and receiver slant stacks. (c) The event is characterized by the travel-time T_{sr} and the ray parameters p_s and p_g and is associated with a ray segment pair in the velocity model. Ray segment parameters including the scatter point location \mathbf{X} , ray shooting angles θ_s and θ_g can be estimated from the half-offset h , the ray parameters, and two-way travel-time T_{sr} .

Comparison of stereotomography methods

CDR tomography uses the picked shot and receiver ray parameters to construct the shot and receiver ray paths and the endpoints of the ray paths; therefore, it is more sensitive to picking errors than the more generalized stereotomography and adjoint stereotomography. Adjoint stereotomography is computationally more efficient than the classical stereotomography because it uses the matrix-free adjoint state method and a much smaller data and model space than the classical stereotomography. Therefore, adjoint stereotomography is an active research topic in stereotomography.

Coupling between scatter point position and velocity

Although the objective of stereotomography is to estimate the velocity model, both classical stereotomography and adjoint stereotomography require the initial estimation and subsequent optimization of scatter point positions. Furthermore, for each pick, there is a scatter point. Therefore, there is no redundancy for the scatter point estimation. There are different methods to estimate the initial scatter point positions (Sword 1987, Billette 1993, Charuis 2002). Adjoint stereotomography uses the gradient of the cost function with

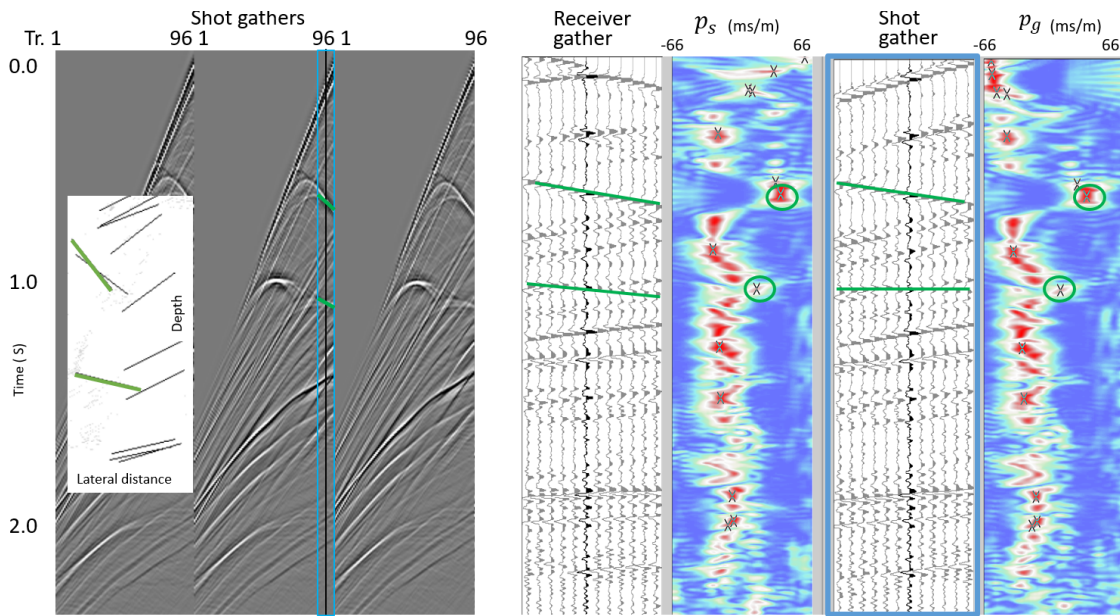


Figure 9. Automatic picking of p_s , p_g and T_{sr} on finite difference synthetic data using the Marmousi Model. The small window on the left shows some initial estimate of the depth and dip of some picks.

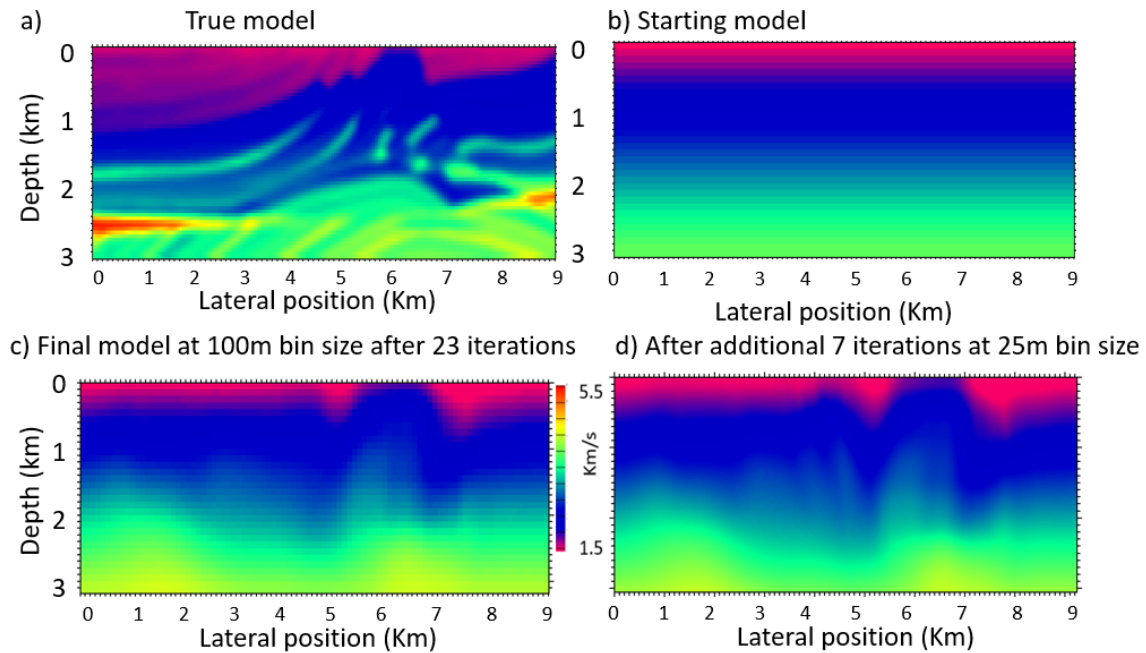


Figure 10. a) true model for adjoint stereotomography test. b) starting model. c) final model after 23 iterations at 100m grid. d) final model after 7 additional iterations at 27m grid.

respect to the scatter point position to update the scatter position; however, there can still be residual errors in the scatter point positions and leads to errors and reduced resolution in the solution of the velocity model. The synthetic test result (figure 10) using the Marmousi model shows that the adjoint stereotomography captures the long-wavelength component of the velocity model. Further investigation into improvements in scatter point

positions estimation is required to improve the resolution of the result from the adjoint stereotomography method.

Sambolian et al. (2018) proposed a Parsimonious stereotomography method that uses the focusing equations of Chauris et al. (2002):

$$T_{n_{sr}}^{obs} = t_s(x_{n_{sr}}) + t_r(x_{n_{sr}}) \quad (15)$$

$$p_r(x_{n_{sr}}) = p_r^{obs}(x_{n_{sr}}) \quad (16)$$

to reconstruct scatter point positions and source slopes. Scatter position $x_{n_{sr}}$ and source slope $p_s(x_{n_{sr}})^{obs}$ for a localized event are computed by matching the focusing equations, where t_s and t_r are computed source and receiver travel-time, p_r is the receiver ray parameter. The data space for this method reduces to source slopes for all the picks, and the model space is reduced to the velocity grid only. Therefore, this does not only reduce the memory and computation requirement but can potentially mitigate the coupling between velocity and scatter point position during the inversion process. However, the accuracy of the scatter positions still depends on the accuracy of the initial velocity model and receiver ray parameter picks. This method will require further investigation.

Picking in model space (depth domain) for stereotomography

Chauris (2002) demonstrated that a picked locally coherent event is characterized by event location (x,z) , offset h , migrated dip ξ , and residual slop ϕ . This allowed more efficient picking because of better coherence in model space. This is followed by a velocity model update step with flatness criteria within the CIG. Similar to PSDM tomography, each update also requires a pass of PSDM.

Guillaume (2008) took the approach of kinematically de-migrating the residual moveout (RMO) and dip picks using the migration velocity to create a set of invariants, T_{obs} , m , h , $slope_m$ and $slope_h$ (Figure 10). These invariants were then used to predict the RMO through kinematic re-migration (Chauris 2002). The RMO prediction and velocity update loop is iterated until RMO is minimized (Figure 11).

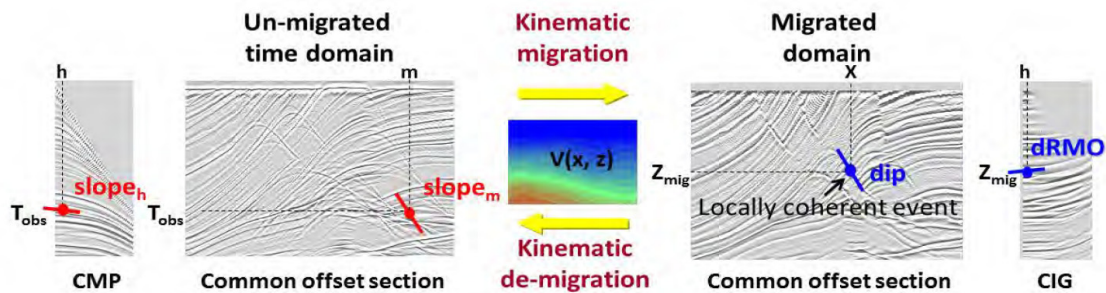


Figure 10. Stereotomography invariants are created via kinematic de-migration using depth, dip, RMO picks in migrated domain. (From Guillaume 2008)

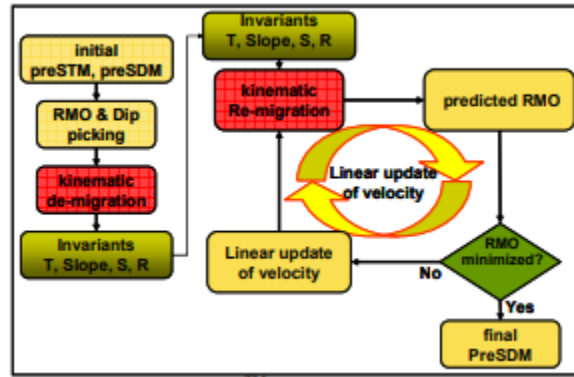


Figure 11. Non-linear depth tomography using invariants from kinematic de-migration of RMO and dip picks. (From Guillaume 2008)

Narrowing the vertical gap between refraction and reflection inversion solution

One problem faced by reflection tomography methods is the lack of reflection data and noise contamination in the near-surface area. Although refraction tomography can provide the near-surface velocity model; however, the depth of illumination for a refraction survey is limited to 1/5 of the maximum offset in the ideal case. To ensure maximum depth of illumination for refraction tomography, the first arrival energy for the far offset traces should be preconditioned to remove any phase variation and noise contamination. Smaller trace spacing and preconditioning can potentially provide better results for reflection tomography solution. This can be a target-based approach. For example, shallow data can be preconditioned to output higher resolution CIG for PSDM tomography, and higher resolution ray-parameter scans for stereotomography.

CONCLUSION

We have reviewed reflection travel-time tomography methods from the classical reflection tomography, to depth migration domain tomography, to stereotomography and adjoint stereotomography. We concluded that picking of reflection travel-times or slopes are difficult and impractical in prestack time domain; while picking in depth migrated domain (model space) for PSDM tomography and in localized slant stacks for stereotomography is more efficient. We also found that non-linear depth tomography using kinematically demigrated RMO and dip picks can be more effective than conventional linear depth migration tomographic methods. Stereotomography inverses jointly the scatter positions and the velocity model. It is an ill posed problem and can potentially compromise the resolution of the solution of the velocity model. Our synthetic test shows that adjoint stereotomography tomography captures the long wavelength component of the true velocity model. We will continue our investigation to improve the resolution of the solution of the velocity model by improving the estimation of the scatter point position. Parsimonious adjoint stereotomography holds the promise of being an efficient algorithm without the problem of parameter cross-talk between velocity and scatter positions. However, it will require further investigation.

ACKNOWLEDGEMENTS

We thank the sponsors of CREWES for continued support. This work was funded by CREWES industrial sponsors, and NSERC (National Science and Engineering Research Council of Canada) through the grant CRDPJ 461179-13.

REFERENCES

- Adler, F., R. Baina, M. Soudani, P. Cardon, and J. Richard. 2008, Nonlinear 3D tomography least-squares inversion of residual moveout in Kirchhoff prestack-depth-migration common image gathers: *Geophysics*, **73**, VE13-VE232008
- Al-Yahya, K., 1989, Velocity analysis by iterative profile migration: *Geophysics*, **54**,718-729.
- Bishop, T. N., K. P. Bube, R. T. Langan, P.L. Love, J. R. Resnick, T. T. Shuey, D. A. Spinder, and H.W. Wyld, 1985, Tomographic determination of velocity and depth in laterally varying media: *Geophysics*, **50**, 903-923.
- Billette, F., and G. Lambaré, 1998, Velocity macro-model estimation from seismic reflection data by stereotomography: *Geophys. J. Int.*, **135**, 671-690.
- Billette, F., S. Le Bé gat, P. Podvin, and G. Lambaré, 2003, Practical aspects and applications of 2D stereotomography: *Geophysics*, **68**, 1008-1021.
- Bording, R., Gersztenkorn, A., Lines, L., Scales, J., and S. Treitel, 1987, Application of seismic travel-time tomography: *Geophys. J. R. astr. Soc.*, **90**, 285-303
- Chauris, H., M. Noble, G. Lambare and P. Podvin, 2002, Migration velocity analysis from locally coherent event in 2-D laterally heterogeneous media, Part I: Theoretical aspects: *Geophysics*, **67**, 1202-1212.
- Chiu, S. and R. Stewart, 1987, Tomographic determination of three-dimensional seismic velocity structure using well logs, vertical seismic profiles, and surface seismic data: *Geophysics*, **52**, 1085-1098.
- Etgen J., F. Billette, R. Sandschaper and W. Rietveld, 2002, The key practical aspects of 3D tomography: data picking and model representation: SEG Technical Program Expanded Abstracts.
- Guillaume. P., G. Lamare, O. Leblanc, P. Mitouard, J. Le Moigne, J. Montel, T. Prescott, R. Siliqi, N. Vidal, X. Zhang and S. Zimine, 2008, Kinematic invariants: an efficient and flexible approach for velocity model building: SEG Technical Program Expanded Abstracts.
- Gray S., S. Cheadle and B. Law, 2000, Depth model building by interactive manual tomography: SEG Technical Program Expanded Abstracts.
- Law B., D. Trad, 2018, Robust refraction statics solution and near-surface velocity model building using feedback from reflection data: *Geophysics*, **83**, U63-U77.
- Lines, L., and R. Newrick, 2004, *Fundamentals of Geophysical Interpretation*: Society of Exploration Geophysicists.
- Sambolian S., Operto, S., Ribodetti, A., Tavakoli F., and Vireux, J., 2018, Parsimonious slope tomography based on eikonal solvers and the adjoint state method: 80th EAGE Conference and Exhibition.
- Stewart, R., 1991, *Exploration Seismic Tomography: Fundamentals*: Society of Exploration Geophysicists
- Stork C., and R. Clayton, 1991, Linear aspects of tomographic velocity analysis: *Geophysics*, **56**, 483-495.
- Stork, C., 1992, Reflection tomography on postmigrated domain: *Geophysics*, **57**, 680-692.
- Sword C. H., 1987, Tomographic determination of interval velocities from reflection seismic data: The method of controlled directional reception. PhD thesis, Stanford University
- Tavakoli F., B., Operto, S., Ribodetti, A. and Vireux, J., 2017, Slope tomography based on eikonal solvers and the adjoint-state method. *Geophysical Journal*, **209**(3), 1629-1647.
- Wang B., K. Pann, R. Meek, 2005, Macro velocity model estimation through model-based globally optimized residual-curvature analysis: SEG Technical Program Expanded Abstracts.
- Woodward, M., D., Nichols, O. ZdraZdraveva, P. Whitfield and T. Johns, 2008, A decade of tomography: *Geophysics*, **72**, VE5-VE11